A Comparison of Relaxation Time Distributions Obtained from Dynamic Light Scattering and Dynamic Mechanical Measurements for High Molecular Weight Polystyrene in Entangled Solutions

Taco Nicolai and Wyn Brown*

Institute of Physical Chemistry, University of Uppsala, Box 532, S-751 21 Uppsala, Sweden

Søren Hvidt and Kurt Heller

Department of Chemistry, Risø National Laboratory and Roskilde University, DK-4000 Roskilde, Denmark

Received February 19, 1990; Revised Manuscript Received May 4, 1990

ABSTRACT: The purpose of this work was to examine possible similarities between the relaxation time distributions for polystyrene in semidilute solutions in the Θ solvent bis(2-ethylhexyl) phthalate (dioctyl phthalate, DOP) obtained from dynamic light scattering (DLS) and dynamic mechanical (DM) measurements. The paper deals mainly with the influence of concentration and molecular weight but also with the role of solvent quality through change in temperature. The DLS and DM relaxation functions have been analyzed by inverse Laplace transformation (ILT) and the DLS data also by fitting the slow, q-independent, part of the spectrum to a general exponential function. It was found that with both techniques the dynamical processes probed at long times are characterized by a similar wide range of relaxation times and that the latter increases strongly with concentration and molecular weight. However, the distribution of relaxation times from DLS is much more sensitive in the slow part of the spectrum to changes in solvent quality.

Introduction

This paper reports results of parallel dynamic light scattering (DLS) and dynamic mechanical measurements (DM) on semidilute solutions of polystyrene (PS) in the viscous solvent DOP, the latter being a Θ solvent at 22 °C. A preliminary report was given in ref 1.

It had earlier been established[2-6] that for PS in a number of Θ systems the autocorrelation functions are strongly non-single-exponential. Laplace inversion analyses[6] show the presence of a broad distribution of relaxation times, all of which are q-independent, in addition to the q^2-dependent diffusional mode characterizing relaxation of the transient network (where q is the scattering vector). Previous papers[5,6] dealt more specifically with the properties of the diffusional mode. The above observation of slowly relaxing components promoted speculation as to their possible sources, one of the alternatives being that the observed relaxation modes in DLS are related to the viscoelastic properties of the network. The purpose here is to examine the similarities and differences between the relaxation time distributions derived from data obtained by using the two techniques. Such an approach is motivated since the relaxation processes occurring in more concentrated systems are plausibly related to the same fundamental disentanglement phenomena. On the other hand, the comparison is not straightforward since the autocorrelation function in DLS ($g_2(t)$) is related to the longitudinal elastic modulus (M) and not directly to the shear modulus (G), the two parameters being coupled through the relationship $M = K + 4/3G$, with K the compressional modulus.[7] The compressional modulus itself is the sum of the osmotic modulus and the elastic modulus of the transient gel. At frequencies much lower than those characteristic of the response of the system to the osmotic force, the relaxation of the system is controlled by the compressional and shear modulus of the transient gel.[27,28,30] Assuming that the frequency dependences of these two moduli are determined by the same dynamic processes (e.g., disentanglement) of the transient gel, they may be very similar. Thus, it seems reasonable to compare the relaxation time dependence of M as measured in DLS at longer times with that of G as determined in dynamic mechanical measurements.

DLS has earlier been used[8-13] in the study of bulk polymer dynamics near and above the glass transition temperature, T_g, where the main contribution to the scattered intensity arises from density fluctuations. The density time correlation function was found to be related to the bulk longitudinal compliance and the relationship verified by measurements on poly(vinyl acetate). The bulk properties depend on local segmental motions associated with the primary glass–rubber transition, and these (in contrast to solution-state properties) are scarcely affected by polymer molecular weight (above a certain minimum) and entanglements. The relaxation spectrum from DLS and DM measurements was found to be a broad single peak, which may or may not correspond to a spectrum of discrete relaxation times.

A major source of differentiation (and complication) between dynamic light scattering and dynamic mechanical measurements is that the autocorrelation function is to a large extent determined by the cooperative relaxation of the transient network, a process that will not be reflected in the dynamic mechanical measurements. Any comparisons between distributions from DLS and viscoelastic measurements are thus restricted to the long time portion of the spectrum. Furthermore, fundamental differences in the manner of data acquisition potentially lead to differences in the relaxation time distributions.

A series of semidilute solutions of high molecular weight PS were prepared in the concentration range 2–14% w/w. Comprehensive DLS measurements were performed, and the same solutions were subsequently used for the dynamic mechanical measurements. This paper deals mainly with the influence of PS concentration and molecular weight on the decay time distributions at the Θ temperature. Experiments have also been made on a selected system as a function of temperature to examine the role of solvent

0024-9297/90/2223-5088$02.50/0

Table I
Properties of the Polystyrene Samples

$M_w/10^6$	M_w/M_n	$C^*/10^{-2}$ (g/mL)	$C_E/10^{-2}$ (g/mL)	$C_J/10^{-2}$ (g/mL)
0.93	1.03	1.66	3.8	15
2.95	1.03	0.93	1.2	4.7
4.9	1.04	0.72	0.71	2.9
8.42	1.05	0.55	0.41	1.6

quality. Since this paper centers on a comparison of the distributions, a major question arises as to the optimal manner of treating the data and the Data Analysis section addresses this aspect.

As with the melts, there is ambiguity as to whether the slower processes correspond to a broad distribution of relaxation times or to an inherently nonexponential relaxation process. We have chosen, however, to analyze the relaxation functions in terms of both an inverse Laplace transformation and a fit to a function in which a single-peaked exponential distribution is used to represent all of the processes slower than the q^2-dependent component.

Apart from this ambiguity in representation, the data from both DLS and DM measurements show a close correspondence regarding the range of slower processes covering several decades on the time scale. This aspect has not earlier been recognized as a major feature in current models for semidilute solutions.

Experimental Section

Polystyrene samples were purchased from Toya Soda except the sample with $M_w = 4.9 \times 10^6$, which was synthesized at Risø National Laboratory and characterized by using light scattering and gel permeation chromatography. Characteristics of the polymer samples used are given in Table I. Solutions were prepared by dissolving polystyrene into Millipore-filtered solvents of analytical grade (Merck, FRG). The solutions were allowed to reach equilibrium, keeping them at 70 °C during a period of several months while regularly turning the sample holders. Concentrations were determined by weight. The error involved by not correcting for the solvent density at different temperatures and concentrations is at most a few percent.[14] Viscosities of DOP have been calculated by using $\ln \eta = -2.46 + 707.9/(T - 188.7)$.[15] The viscosity of di-*n*-butyl phthalate (DBP) at 25 °C was found to be 0.166 P.

The concentration, C^*, separating the dilute from the semidilute regime is taken to be equal to $3M_w/4\pi R_g^3 N_A$, i.e., the concentration where the polymer coils start to overlap. Here R_g is the radius of gyration and N_A is Avogadro's number. Experimentally the relationship between the radius of gyration and the molecular weight of polystyrene in Θ solutions has been found to be $R_g = 0.29M^{0.5}$ Å.[16] Two concentrations that characterize the onset of the effect of topological constraints or entanglements are C_E and C_J. C_E is the concentration at which entanglements begin to influence the viscosity of the solution, and C_J is the concentration at which the steady-state compliance becomes independent of the molecular weight. Experimentally it has been found that for polystyrene $C_E = 3.6 \times 10^4/M_w$ g/mL and $C_J = 1.4 \times 10^5/M_w$ g/mL.[17,18] Values of these critical concentrations for the polystyrene samples used are given in Table I.

The experimental arrangement to perform DLS measurements has been described previously.[3] The light source was a 633-nm He–Ne laser. An ALV Langen Co., multibit, multi-τ autocorrelator was operated with 23 simultaneous sampling times (covering, for example, delay times in the range 1 μs to 1 min) in the logarithmic mode and 191 channels. The stability of the photon count indicated the solutions were essentially dust-free.

A Rheometrics RFS8500 instrument with a fluid bath temperature control (±0.1 °C) was used for oscillatory shear measurements. A cone and plate geometry cell (diameter 50 mm, angle 0.02 rad) was used for most measurements. A parallel plate (diameter 50 mm) was used for the highest concentrations and a couette geometry (inner diameter 16 mm, outer diameter 17 mm, length 45 mm) for the lowest concentrations. Samples of high viscosity were kept warm during this transfer with the aid of a heat jacket maintained at 70 °C. The storage and loss moduli, G' and G'', were measured as a function of angular frequency between 10^{-3} and 10^2 rad/s. A total of 5–10 points/decade were measured. The strain amplitude dependence of the viscoelastic data was checked for several samples, and measurements were only performed in the linear range where moduli are independent of strain amplitude. Typical strain amplitudes were varied between 1 and 50% depending on concentration and molecular weight.

Data Analysis

DLS Data. For the analyses of the correlograms two basically different methods were applied. In the first instance an inverse Laplace transformation (ILT)

$$g_1(t) = \int_0^\infty w(\tau)\, e^{-t/\tau}\, d\tau \qquad (1)$$

of the data was performed by using a constrained regularization calculation routine called REPES[19] to obtain a distribution $w(\tau)$ of relaxation times as described elsewhere.[6] The range of relaxation times allowed in the fit usually extended the range of delay times, t, by a factor of 10 at the fast and slow ends. A grid density of about 10 points/decade was used. This method yields in all cases an almost perfect fit to the data, showing no systematic deviation in the residuals. In general, the distributions obtained in this way show one fast peak, the position of which changes with changing scattering vector, q, and a number of slower peaks independent of q. Two other calculation routines to perform the Laplace inversion (MAXENT[20,21] and CONTIN[22]) were tried on several correlograms and gave very similar results. The detail of the relaxation time distributions is usually preserved even if a large amount of smoothing is allowed (see Figure 2 or ref 6).

In order to see to what extent the apparently discrete nature of the slow modes is forced by the data, the correlograms were also fitted to a sum of two distributions. One is Gaussian in log τ and represents the fast q-dependent peak:

$$w_1(\tau) = \exp\left(-\left\{\frac{\log(\tau/\tau_d)}{\sigma}\right\}^2\right) \qquad (2)$$

The other is a so-called generalized exponential (GEX) distribution representing the total of all the slow peaks[23]

$$w_2(\tau) = |s|\tau^{ps-1}\tau_0^{-ps} \exp(-\{\tau/\tau_0\}^s)/\Gamma(p/s) \qquad (3)$$

with p and s both taken as positive, τ_d and τ_0 are relaxation times that position $w_1(\tau)$ and $w_2(\tau)$ on the time axis, σ characterizes the width of the Gaussian distribution, and the parameters p and s determine the shape of the GEX distribution. In the absence of a theoretical model predicting a specific form, w_2 was chosen to represent the total of the slow modes by a single-peaked distribution with a large freedom in shape. Since the purpose of this second analytical approach is only to determine to what extent a single-peaked distribution of slow relaxation processes is consistent with the experimental data, physical significance is not placed on the individual parameters determining the shape of w_2. The results from the ILT show that the fast q^2-dependent peak limits the distribution on the fast side (except for a small contribution of internal modes). This can be clearly seen from the distributions at different values of the scattering vector (see Figure 6 of ref 6). Therefore, it is necessary to cut off $w_2(\tau)$ at the fast end where it overlaps with $w_1(\tau)$. The cut-off function

used here is rather arbitrary, but the influence of the exact shape of the cut-off function on the total relaxation time distribution ($w(\tau)$) is small since $w_1(\tau)$ is narrow and $w_2(\tau)$ is in most cases small where it starts to overlap with $w_1(\tau)$. The total relaxation time distribution is calculated as

$$w(\tau) = A_1 w_1(\tau) + A_2 w_2(\tau)\, F(\tau) \tag{4}$$

with the cut-off function given by

$$\begin{aligned} F(\tau) &= 1 && \log \tau > \log(\tau_d) + \sigma \\ &= \log(\tau/\tau_d)/2\sigma + 0.5 && \log(\tau_d) - \sigma \geq \log \tau \geq \log(\tau_d) - \sigma \\ &= 0 && \log \tau < \log(\tau_d) - \sigma \end{aligned} \tag{5}$$

The two individual distributions that make up $w(\tau)$ are normalized to unity through division by $\int_0^\infty w_1(\tau)\, \mathrm{d} \log(\tau)$ and $\int_0^\infty w_2(\tau)\, F(\tau)\, \mathrm{d}\tau$, respectively, so that A_1 and A_2 are relative contributions to $w(\tau)$. The intensity autocorrelation function that is used in the fitting is calculated as

$$g_2(t) = a g_1(t)^2 + b \tag{6}$$

where $g_1(t)$ is given by eq 1 and $w(\tau)$ is given by eq 4. $g_2(t)$ calculated in this way is thus characterized by eight parameters $(a,b,(A_1/A_2),\tau_0,\tau_d,p,s,\sigma)$, which were all allowed to float during the fitting. The range of relaxation times allowed in the fitting and the density per decade was similar to that used in the calculation of the inverse Laplace transform. The general shape of the relaxation time distributions obtained in this way is very similar to the results from ILT but with the slow modes replaced by a smooth broad distribution. The residuals to the fit, however, are not random, especially at shorter delay times, but the absolute deviations are never more than 0.5% of $g_2(t)_{max}$. Possible reasons for the systematic deviations are the effect of short relaxation times due to internal modes and the choice of the cut-off function.

The two ways of analyzing the correlograms are illustrated in Figures 1 and 2. The weighted residuals from the ILT are clearly random (see Figure 1d) while the unweighted residuals (see Figure 1c) show that the noise on the correlograms increases with increasing delay times. The latter is due to a worsening of the statistics of the correlation at longer delay times and illustrates the necessity of extended time measurements if long decay times are probed. Therefore, the measurements were performed over time periods between 15 and 40 h. It is thus the mere length of the measuring time that is needed to reduce the noise on the correlogram at long delay times, which effectively limits the practical application of the DLS technique. Spontaneous concentration fluctuations are much more extended in Θ solutions and become infinite at the critical point. The method is thus effectively limited by its ability to measure the response of the system to these large-scale fluctuations which are exceedingly slow for high molecular weights and at high concentrations.[34] The second analysis method (see Figure 2) shows nonrandom residuals at shorter delay times that are much larger than those from the ILT, but at longer delay times the residuals are quite similar in magnitude. It seems that the use of a continuous, smooth distribution is sufficient for a good fit to the slow part of the correlogram.

Simulations have shown that the calculation routines used to perform the ILT have a tendency to split a broad asymmetric peak into several narrower peaks especially when another narrow peak is present.[23] To see whether this is the case here, a correlogram was simulated by using the relaxation time distribution from the second analysis

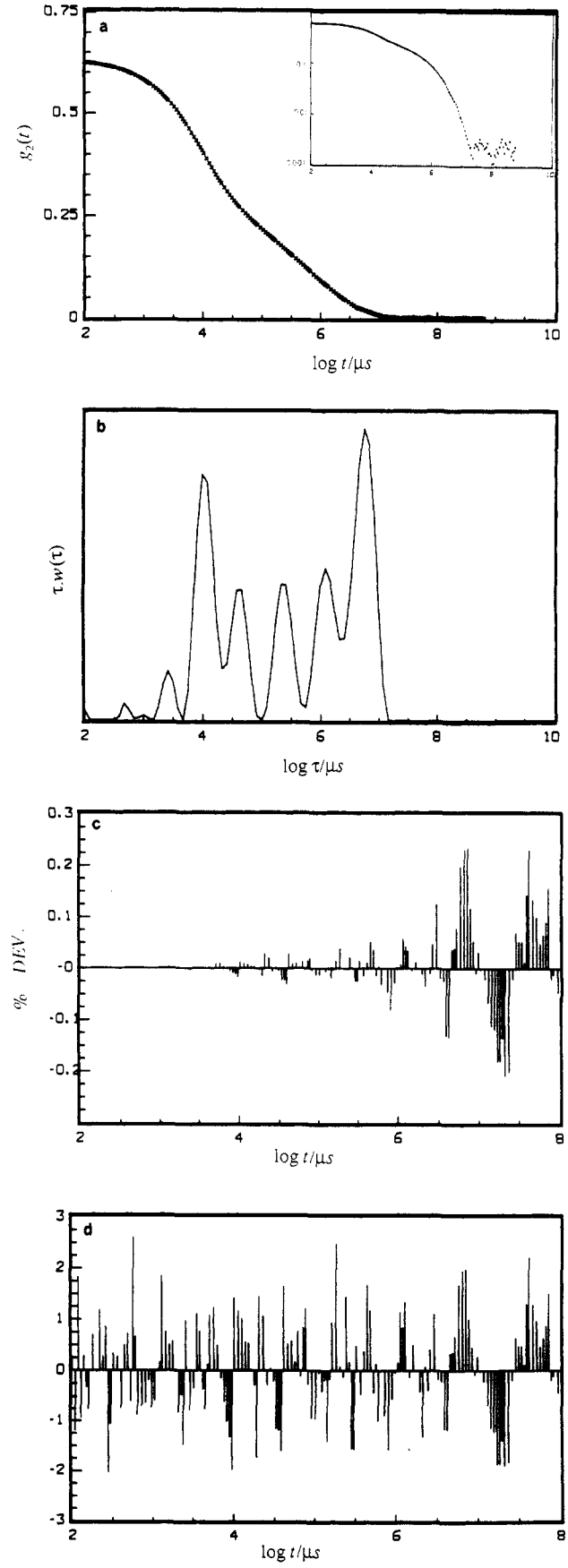

Figure 1. Experimental correlation function (a) with its relaxation time distribution obtained by using REPES (b) for polystyrene in DOP at 22 °C. A log–log version of the data is shown in the inset. $M_w = 4.9 \times 10^6$, $C = 2.78 \times 10^{-2}$ g/mL, and $q^2 = 7.0 \times 10^{14}$ m^{-2}. The residuals are shown as a percentage of $g_2(t)_{max}$ in part c and the weighted residuals are shown in part d for which 66% are expected to fall between −1 and +1.

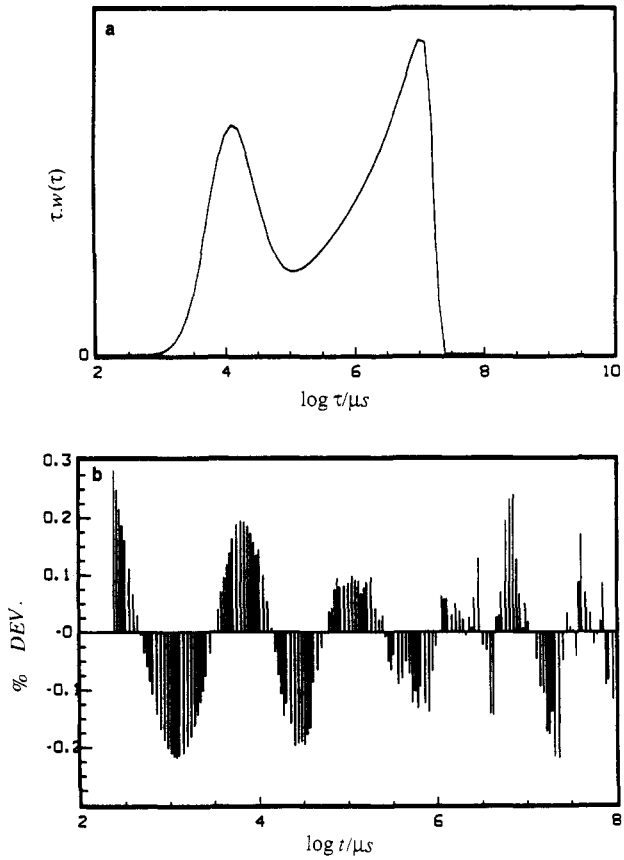

Figure 2. Relaxation time distribution obtained from a forced fit to a sum of a Gaussian and a GEX distribution to the correlogram shown in Figure 1a. The residuals are shown as a percentage of $g_2(t)_{max}$ in part b.

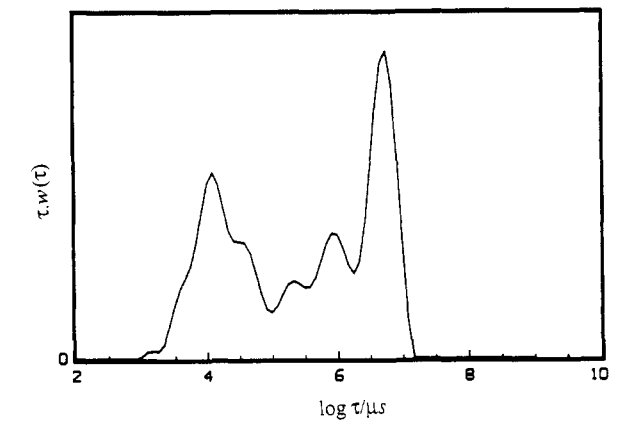

Figure 3. Relaxation time distribution obtained by using REPES of a simulated correlation function for which the relaxation time spectrum shown in Figure 2a is used with the experimental noise shown in Figure 1c added.

method (see Figure 2a). If no noise is added to the simulated correlogram, an inverse Laplace transform yields a relaxation time distribution identical with that used in the simulation. If an increasing amount of random noise is added, the broad asymmetric peak shows an increasing tendency to split up into several peaks. However, this tendency is not sufficient to explain the detail at the slow end of the distribution obtained from an ILT of the experimental data. This can be demonstrated by adding the experimental noise shown in Figure 1c to the simulated correlogram. In this case the distribution shows a weaker modification of the broad asymmetric peak (see Figure 3). On the other hand, a very small amount of systematic noise in the experimental correlogram could cause a stronger modification of the broad peak. Such systematic noise would not show up in the residuals and therefore is not put into the simulated correlogram. We conclude that by representing the total of the q-independent slow modes by a single broad asymmetric peak the experimental data can be described with high accuracy and that the detail obtained from an ILT may possibly be caused by external disturbances. It is noted that these disturbances are related to long time correlation since measurements on a static scatterer (glass) yield the expected Poisson noise.

Dynamic Mechanical Data. The stress relaxation shear modulus, $G(t)$, was calculated from G' and G'' by use of the approximate expression of Ninomiya and Ferry (see eq 48, Chapter 4 of ref 17)

$$G(t) = G'(\omega) - 0.4G''(0.4\omega) + 0.014G''(10\omega) \quad (7)$$

which uses G' at the frequency $\omega = 1/t$ and G'' at two other frequencies. The error that is introduced by the use of this approximation is a small fraction of $G''(\omega)$.[24] Direct evaluation of $G(t)$ by Fourier transformation gives much worse results because only a limited range of frequencies is experimentally accessible. Corresponding relaxation time distributions were obtained by performing an ILT of $[G(t)]^2$ data in the same way as for the DLS data. Often $\log w(\tau)$ is plotted versus $\log \tau$ in the literature when relaxation time distributions obtained from DM measurements are presented. Here, we have chosen an equal area representation by plotting $\tau w(\tau)$ versus $\log \tau$ in line with DLS literature. Good fits showing random residuals were obtained if the $G(t)$ values at the two shortest times were not included in the fit. For the more concentrated solutions ($C > 6 \times 10^{-2}$ g/mL) it was necessary to exclude more $G(t)$ values at the short times as the rheometer used does not respond properly at the highest frequencies for the most viscous solutions. In general, broad distributions are obtained that show much less detail than the distributions obtained using ILT of the DLS data. We need to keep in mind, however, that the shape of $w(\tau)$ at short relaxation times ($\tau < t_{min} \approx 10^{-4}$ s) is determined here by the limited time range of $G(t)$. The distributions obtained from DLS are not perturbed in this way as the time range of $g_2(t)$ is much wider and $w(\tau)$ is always close to zero at the shortest delay times measured. An example of $G(t)$ calculated by using eq 7 is shown in Figure 4a together with $G'(t)$ and $G''(t)$. The corresponding relaxation time distribution obtained from an ILT is shown in Figure 4b by the dotted line. For comparison distributions obtained by using more approximate methods directly from $G'(\omega)$ and $G''(\omega)$ are shown also, where eqs 12 and 26 of Chapter 4 in ref 17 have been used to calculate the respective distributions. From a comparison of the residuals to the fit it is clear, however, that these methods yield a much poorer fit to the data (see parts c and d of Figure 4). In addition, simulations show that these methods do not resolve discrete relaxation times that differ by less than a factor of 10 even if no noise is present in the data. Therefore, lacking a model to which the data can be fitted directly, ILT of the data using a constrained regularization routine is probably the best way to obtain $w(\tau)$ from the dynamic mechanical measurements.

Results and Discussion

Parallel DLS and DM measurements have been performed on semidilute solutions of polystyrene in DOP as a function of concentration and molecular weight. For one solution the dependence on the solvent quality has been investigated by varying the temperature while correcting for changes in the solvent viscosity and the kinetic energy. As a limiting case the sample has been measured in dibutyl phthalate (DBP) at 25 °C, for which the solvent quality

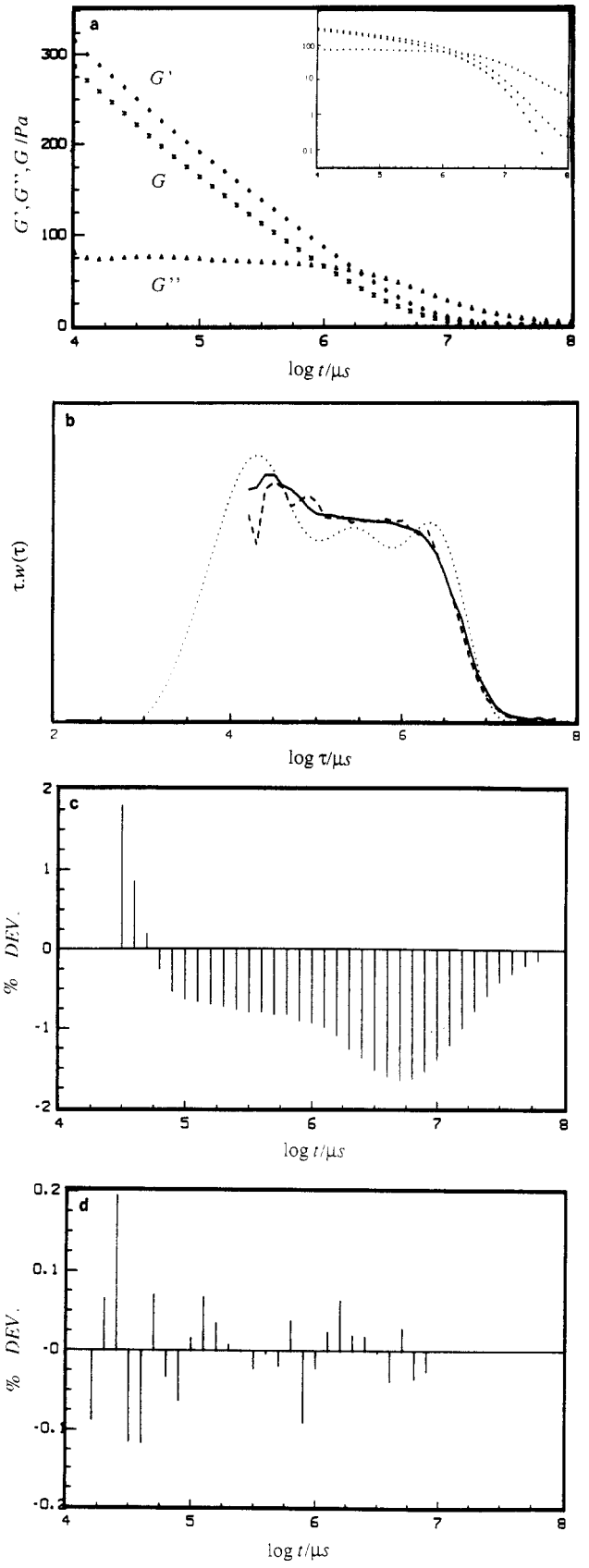

Figure 4. Experimental values of G' (diamonds) and G'' (triangles) together with G calculated via eq 7 (crosses) of polystyrene in DOP at 22 °C. ($M_w = 2.95 \times 10^6$, $C = 5.75 \times 10^{-2}$ g/mL.) The relaxation time distributions obtained by using REPES (dotted) and two other methods (see text) are shown in part b (dashed line, eq 26, Chapter 4, ref 17; full line, eq 12, Chapter 4, ref 17). The residuals corresponding to the distributions given by the solid and dotted lines are shown as a percentage of $G(t)_{max}$ in parts c and d, respectively. The inset to Figure 4a shows the same data on a log–log scale.

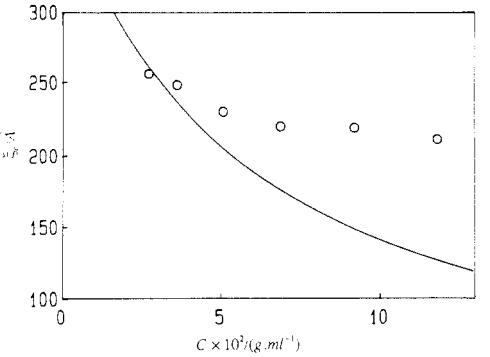

Figure 5. Comparison of the concentration dependence of the dynamic correlation length of polystyrene in DOP at 22 °C (circles) with that in cyclohexane at 35 °C (solid line) in the semidilute regime.

is intermediate between a Θ solvent and a good solvent.[25] Here we will concentrate on the comparison of the relaxation time distributions obtained from the two different experimental techniques. A detailed treatment of the viscoelastic data will be given elsewhere.

The DLS results were obtained at a single angle after establishing the q independence of D and the q independence of the slow relaxation times described in the analogous polystyrene/cyclohexane system[6] and as illustrated in Figure 1a. The scattering vectors used are given in the appropriate figure captions.

As described in the previous section, relaxation time distributions have been obtained from both types of dynamical measurements. These distributions enable us to compare the dynamical processes that are probed by these two techniques as a function of C, M_w, and solvent quality. The fast diffusional mode, which is observed in the DLS spectra, has been discussed elsewhere for a very similar system (polystyrene in cyclohexane).[5,6] Reanalysis of those data using a forced fit to a sum of a Gaussian and a GEX distribution confirmed the general conclusions that were drawn there with respect to the diffusional mode and the range of the slower modes; see Appendix. Especially, the q-independence of the latter is very clear if this analysis method is used; see Figure 12. For that system it was found that the effective dynamic correlation length, ξ_e, calculated from the cooperative diffusion coefficient, D_c, via $\xi_e = kT/6\pi\eta_s D_c$, decreases weakly with increasing C, is independent of M, and decreases with increasing solvent quality due to the increasing influence of binary thermodynamic interactions.[26] ξ_e defined in this way is not identical with the hydrodynamic correlation length ξ_h but combines the effect of hydrodynamic screening and the elasticity of the transient gel, as discussed elsewhere.[6] The concentration dependence at Θ conditions could be explained, following a theory by Brochard and de Gennes,[27,28] by assuming an interplay between elastic forces in the transient network and ternary thermodynamic interactions. The dynamic correlation lengths calculated for the polystyrene/DOP system show the same qualitative dependences. However, the decrease of ξ_e with increasing concentration is much smaller in DOP than in cyclohexane or cyclopentane at their respective Θ temperatures. In Figure 5 values of ξ_e calculated from the fast peak in the ILT spectra in DOP are plotted as a function of the concentration and compared with the behavior in cyclohexane. (Values of ξ_e calculated from τ_d, see eq 2, are systematically about 10% smaller.) The decrease of the relative amplitude of the diffusional mode with increasing concentration is also smaller in DOP. The reason for these differences may be that the third vir-

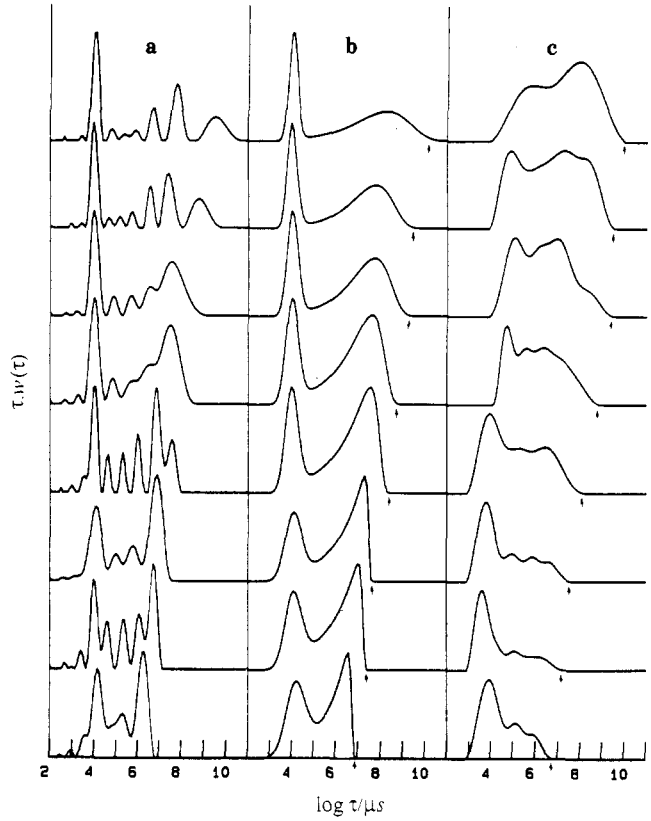

Figure 6. Relaxation time distributions obtained from DLS (a,b) and DM (c) measurements of polystyrene in DOP at 22 °C (M_w = 4.9 × 10^6) at various concentrations. The data have been analyzed by using REPES (a,c) and a forced fit to a sum of a Gaussian and a GEX distribution (b). Final relaxation times are indicated by arrows. From top to bottom the concentrations are 14.5, 11.8, 9.18, 6.82, 5.06, 3.62, 2.73, and 2.19 × 10^{-2} g/mL. q^2 = 7.0 × 10^{14} m^{-2}.

ial coefficient is smaller in DOP. Another possibility is that the assumption that the solvent viscosity is the only determining factor for local segment friction over the whole concentration range measured is not valid in DOP. In this context it is noted that the reduced temperature, $T_{red} = (T - \theta)/T$, at which polystyrene precipitates is much lower in DOP than in cyclohexane or cyclopentane at the same concentration in both the dilute[29] and semidilute regimes. Nevertheless, the general shape of the relaxation spectra obtained from measurements in different solvents is very similar.

Figure 6 shows relaxation time distributions obtained from DLS and DM measurements on polystyrene (M_w = 4.9 × 10^6) in DOP at 22 °C over a range of concentrations above the entanglement concentration. A large scattering vector (q^2 = 7.0 × 10^{14} m^{-2}) has been used in the DLS measurements in order to shift the q-dependent peak toward the fast end of the spectrum. For each concentration three spectra are shown: two from the different analyses of the DLS data and one from the DM data. Ignoring for the moment the contribution of diffusion, one obtains a broad distribution of relaxation times from both DLS and DM measurements. (The detail in the first distribution at each concentration is possibly caused by a small amount of systematic noise on the correlogram as was discussed in the preceding section.) It is clear that the range of relaxational modes probed by the two experimental techniques is very similar at the slow end of the spectra. As was explained in the preceding section, the fast end of the spectra cannot be compared due to the effect of diffusion in DLS and the limited range of frequencies accessible in DM measurements. For a more

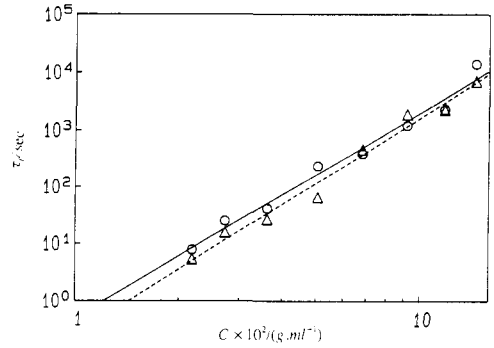

Figure 7. Concentration dependence of the final relaxation times from DLS (circles) and DM (triangles) measurements (arrows in Figure 6). (DOP at 22 °C; M_w = 4.9 × 10^6.)

quantitative comparison one may arbitrarily define a final relaxation time, τ_f, as the longest time that gives a significant contribution to $w(\tau)$. The values of τ_f have been estimated from Figure 6 as indicated by arrows and are plotted on a logarithmic scale against C in Figure 7. The final relaxation time taken in this way appears to increase exponentially with C. Assuming $\tau_f \sim C^\nu$, $\nu = 3.6 \pm 0.2$ from DLS and $\nu = 3.8 \pm 0.2$ from DM. These values differ appreciably from other values for Θ systems reported in the literature, viz., $\nu = 4.5$[18] for polystyrene in DOP at 25 °C and $\nu = 2.8$[30] for polystyrene in cyclohexane at 35 °C. However, different methods were used to obtain the final relaxation time in these cases.

The general shape of the spectra, i.e., a broad distribution over several decades of relaxation times, is not predicted theoretically. From viscoelastic theory one expects to find two relaxational modes: a slow mode due to disentanglement of the chains and a fast mode due to internal dynamics of parts of the chains between two entanglements.[18] The effect of internal modes on the autocorrelation function has been discussed elsewhere[31] but is small since $R_g q < 1$ in all DLS measurements reported here if we take for R_g the radius of gyration of a part of the chain between two entanglements. The latter may be estimated by assuming that the molecular weight between two entanglements, M_e, is inversely proportional to the volume fraction of the polymer using $M_e \approx 1.8 \times 10^3$ [18] for polystyrene melts. The slowest internal mode for single coils probed in DM measurements may be calculated by using[32]

$$\tau_1 = 0.42 M_w \eta_s [\eta]/RT \quad (8)$$

where non-free-draining hydrodynamic interactions are assumed. Here R is the gas constant and $[\eta]$ is the intrinsic viscosity. For a single polystyrene chain with M_w = 4.9 × 10^6, $\tau_1 \approx 2 \times 10^4$ μs where $[\eta] = 0.091 M_w^{0.5}$ mL/g[33] has been used.

Equation 8 may also be used for semidilute solutions if we use the molecular weight of the part of the chain between entanglements, which decreases with increasing concentration.[17] Thus 2 × 10^4 μs is an upper limit for the relaxation times of the internal modes. Possible effects of hydrodynamic screening will be relatively small on a logarithmic scale.

It is concluded, therefore, from both the DLS and DM measurements that in semidilute polymer solutions a broad range of relaxational modes exists that cannot be attributed to internal modes of parts of chains between two entanglements. Furthermore, we cannot speak of a characteristic terminal relaxation time other than as the relaxation time of the slowest dynamical process, giving a significant contribution to the response of the system

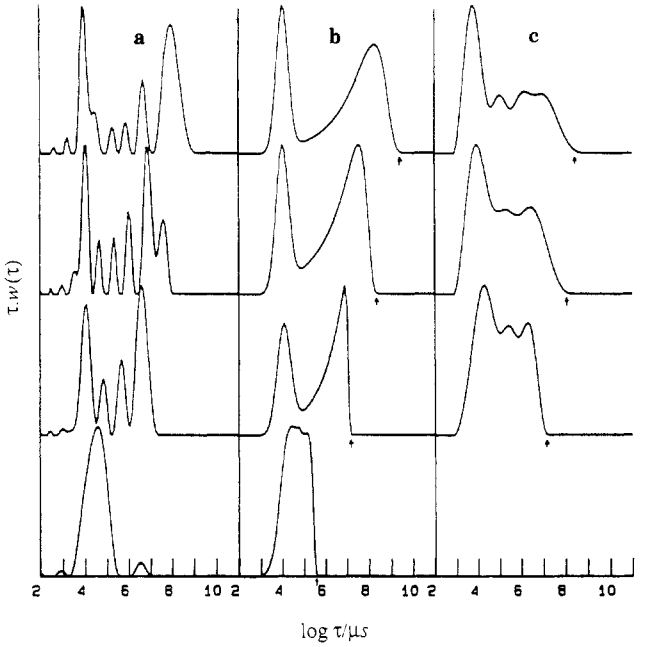

Figure 8. Relaxation time distributions obtained from DLS (a,b) and DM (c) measurements of polystyrene in DOP at 22 °C ($C \approx 5.5 \times 10^{-2}$ g/mL) of various molecular weights. The data have been analyzed by using REPES (a,c) or a forced fit to a sum of a Gaussian and a GEX distribution (b). Final relaxation times are indicated by arrows. From top to bottom the molecular weights are 8.42, 4.9, 2.95, and 0.93×10^6. $q^2 = 7.0 \times 10^{14}$ m^{-2}.

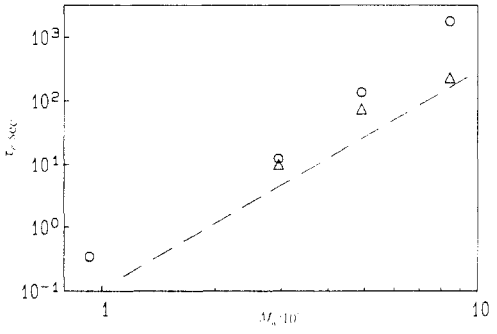

Figure 9. Molecular weight dependence of the final relaxation times from DLS (circles) and DM (triangles) measurements. A line with slope 3.4 is drawn for comparison (see text).

to either spontaneous concentration fluctuations (DLS) or mechanical deformation (DM). On comparison of the shape of the distributions obtained from DLS with those obtained from DM measurements, it is clear that if the same dynamical processes are being probed, as suggested by the similar relaxation time ranges, the sensitivity of the method to these processes is markedly different; DLS weights the slower processes more strongly. A speculative explanation for this difference will be given when discussing the solvent quality dependence.

In Figure 8 relaxation time distributions are plotted for various molecular weights at a fixed concentration ($C \approx 0.05$ g/mL) and show a strong increase of τ_f with increasing molecular weight; see Figure 9. For the lowest molecular weight $G(t)$ has not been calculated because the damping of this system is too strong for eq 7 to be valid. In concentrated solutions and melts one usually observes that the so-called terminal relaxation time increases with $M_w^{3.4}$. In view of the limited amount of data no attempt has been made to establish a scaling relation between τ_f and M_w, but a straight line with slope 3.4 is drawn in Figure 9 to show the qualitative agreement of our findings in semidilute solutions and this slope.

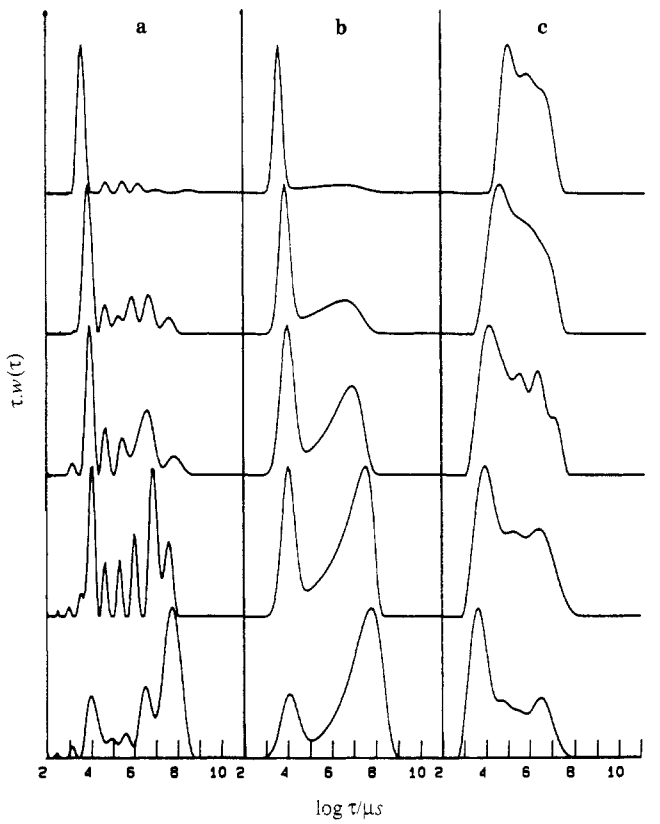

Figure 10. Relaxation time distributions obtained from DLS (a,b) and DM (c) measurements of polystyrene in DOP ($M_w = 4.9 \times 10^6$, $C = 5.06 \times 10^{-2}$ g/mL) at various temperatures and in DBP at 25 °C (top). The data have been analyzed by using REPES (a,c) or a forced fit to a sum of a Gaussian and a GEX distribution (b). The relaxation times have been reduced to DOP at 22 °C by multiplying τ with $(\eta_{(DOP,22°C)}T/\eta_{295})$. From top to bottom the temperatures are 25 (DBP), 45, 30, 22, and 15 °C. $q^2 = 7.0 \times 10^{14}$ m^{-2}.

Relaxation time distributions as a function of solvent quality (temperature) at a fixed concentration and molecular weight ($C \approx 0.05$ g/mL and $M_w = 4.9 \times 10^6$) are shown in Figure 10. The changes with solvent quality are dramatic for the DLS measurements but small for the DM measurements. The small change in the latter case indicates that thermodynamic interactions are not very important in the response of the system to comparatively large-scale mechanical deformation. In the case of DLS the relative contribution of the q-independent modes to the correlogram decreases strongly with increasing solvent quality while the total scattered light intensity also decreases. This may be attributed to increasing thermodynamic interactions, which decrease the amplitude of the spontaneous concentration fluctuations. In order to remove this effect on the relative amplitudes, the spectra are given in Figure 11 without the diffusional peak. From Figure 11 it is clear that apart from a general decrease in amplitude of the slow modes there is also a change in the shape of the distribution. If the solvent quality is worse, the relaxation time distribution is more asymmetric with a relative stronger contribution of the slower times. A possible explanation for this phenomenon could be that the largest concentration fluctuations, which scatter the most light, decay with the slowest relaxation times. If the solvent quality is increased, large concentration fluctuations become less probable due to increasing thermodynamic interactions. In DM measurements no such preferential probing of the slowest dynamical processes occurs.

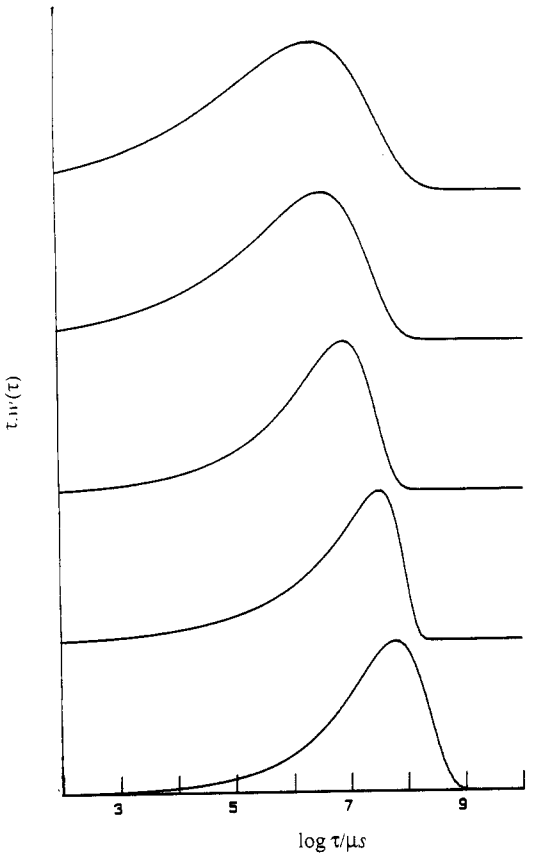

Figure 11. Relaxation time distributions as in Figure 10b but showing only the GEX distributions that represent the total of all q-independent modes.

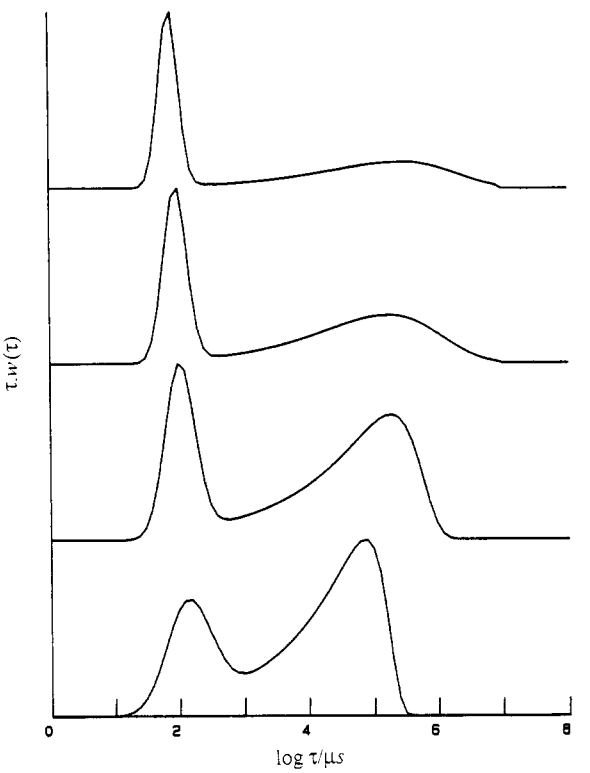

Figure 13. Relaxation time distributions obtained from DLS measurements on a semidilute solution of polystyrene in cyclohexane at 35 °C ($M_w = 3.8 \times 10^6$, $q^2 = 7.0 \times 10^{14}$ m^{-2}) for different polymer concentrations using forced fits to a sum of a Gaussian and a GEX distribution. From bottom to top C is 3.7, 6.4, 10.2, and 12.6 × 10^{-2} g/mL.

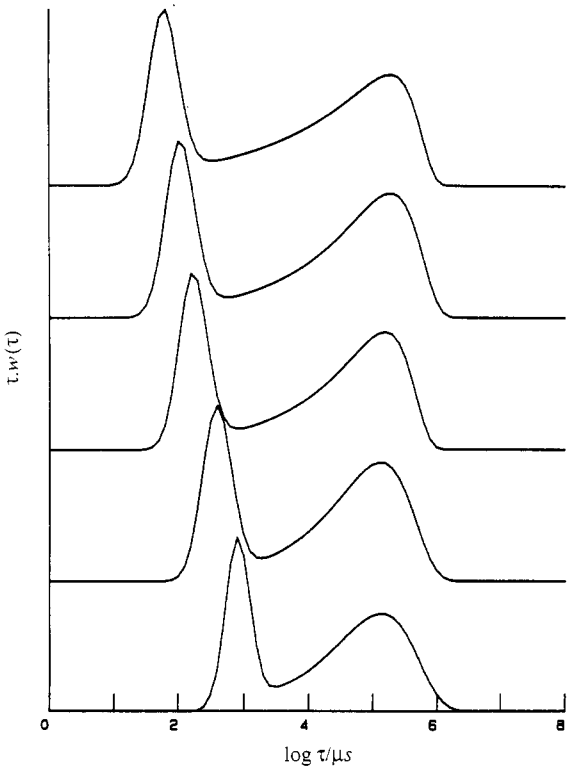

Figure 12. Relaxation time distributions obtained from DLS measurements on a semidilute solution of polystyrene in cyclohexane at 35 °C ($M_w = 3.8 \times 10^6$, $C = 6.4 \times 10^{-2}$ g/mL) at various scattering vectors using forced fits to a sum of a Gaussian and a GEX distribution. From bottom to top q^2 = 0.93, 2.0, 4.0, 7.0, and 11.8 × 10^{14} m^{-2}.

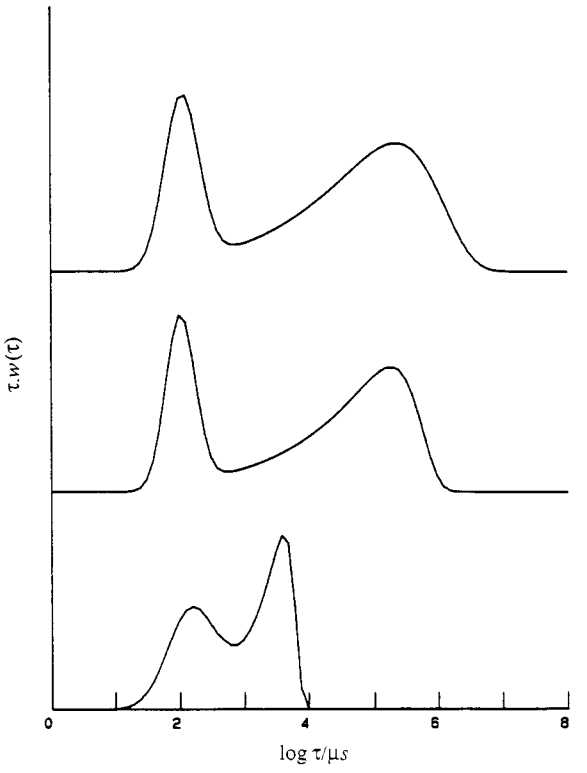

Figure 14. Relaxation time distributions obtained from DLS measurements on a semidilute solution of polystyrene in cyclohexane at 35 °C (~6.5 × 10^{-2} g/mL, $q^2 = 7.0 \times 10^{14}$ m^{-2}) of different molecular weights using forced fits to a sum of a Gaussian and a GEX distribution. From bottom to top M_w is 1.28, 3.8, and 5.48 × 10^6.

Conclusions

The following conclusions may be drawn from the parallel DM and DLS measurements that are reported in this paper:

(1) In both DM and DLS measurements on semidilute polymer solutions in Θ solvents dynamical processes are probed that are characterized by a wide range of relaxation times.

(2) The relaxation time range at long times is in most cases the same for both techniques if the same solution is measured and increases strongly with increasing concentration and molecular weight.

(3) The sensitivity to the dynamic processes that are occurring is different for the two techniques, with DLS being more sensitive to slower processes.

(4) Relaxation time distributions obtained from DM measurements do not change much with changing solvent quality, while the spectra obtained from DLS measurements show a dramatic change in the relative contribution of the various relaxational modes.

(5) The cooperative diffusion coefficient of polystyrene in DOP is different from that in cyclohexane and cyclopentane but has the same qualitative dependence on the concentration, molecular weight, and temperature.

It is clear that further experimental and theoretical work is needed for an understanding of the dynamics of semidilute polymer solutions. It would be especially interesting to extend these measurements to higher concentrations in order to see whether there is a smooth transition to the case of melts above the glass transition temperature for which a more direct relationship between spectra obtained from DLS and DM measurements has been established.[8-13] Much lower molecular weights will have to be used, though, because the relaxational processes of the high molecular weight samples used here will become too slow to be experimentally accessible. Such studies are in progress.

Acknowledgment. We thank Drs. J. Jakeš and R. M. Johnsen for assistance with programs used in this work. The authors are grateful to Dr. K. Almdal for the supply of polystyrene samples. This work was supported by the Swedish Natural Science Research Council (W.B.) and the Danish Natural Science Research Council (S.H.).

Appendix

Results from DLS measurements on polystyrene in cyclohexane at 35 °C, which were published earlier,[4] have been reanalyzed by using a forced fit to a sum of a Gaussian and a GEX distribution; see Data Analysis. Relaxation time distributions are shown as a function of q^2 in Figure 12, C in Figure 13, and M_w in Figure 14. These figures may be compared to Figure 6 and parts a and b of Figure 8 of ref 4, where the results from an inverse Laplace transform analysis are shown.

References and Notes

(1) Brown, W.; Nicolai, T.; Hvidt, S.; Štěpánek, P. *Macromolecules* **1990**, *23*, 357.
(2) Adam, M.; Delsanti, M. *Macromolecules* **1985**, *18*, 1760.
(3) Brown, W. *Macromolecules* **1986**, *19*, 387, 3006.
(4) Brown, W.; Johnsen, R. M.; Štěpánek, P.; Jakeš, J. *Macromolecules* **1988**, *21*, 2859.
(5) Nicolai, T.; Brown, W. *Macromolecules* **1990**, *23*, 3150.
(6) Nicolai, T.; Brown, W.; Johnsen, R. M.; Štěpánek, P. *Macromolecules* **1990**, *23*, 1165.
(7) Tanaka, T.; Hocker, L. O.; Benedek, G. B. *J. Chem. Phys.* **1973**, *59*, 5151.
(8) Wang, C. H.; Fisher, E. W. *J. Chem. Phys.* **1985**, *82*, 632, 4332.
(9) Wang, C. H.; Fytas, G.; Fisher, E. W. *J. Chem. Phys.* **1985**, *82*, 4332.
(10) Fytas, G.; Wang, C. H.; Fisher, E. W. *Macromolecules* **1985**, *18*, 1492.
(11) Hagenah, J. U.; Meier, G.; Fytas, G.; Fisher, E. W. *Polym. J.* **1987**, *19*, 441.
(12) Meier, G.; Hagenah, J. U.; Wang, C. H.; Fytas, G.; Fisher, E. W. *Polymer* **1987**, *28*, 1640.
(13) Fytas, G.; Ngai, K. L. *Macromolecules* **1988**, *21*, 804.
(14) Park, J. O.; Berry, G. C. *Macromolecules* **1989**, *22*, 3022.
(15) Štěpánek, P. Thesis, Charles University, Prague, 1981.
(16) Schmidt, M.; Burchard, W. *Macromolecules* **1981**, *14*, 210.
(17) Ferry, J. D. *Viscoelastic Properties of Polymers*, 3rd ed.; Wiley: New York, 1980.
(18) Takahashi, Y.; Noda, I.; Nagasawa, M. *Macromolecules* **1985**, *18*, 2220.
(19) Jakeš, J., unpublished results.
(20) Livesey, A. K.; Delaye, M.; Licinio, P.; Brochon, J. E. *Faraday Discuss. Chem. Soc.* **1987**, *83*, 247.
(21) Livesey, A. K.; Delaye, M.; Licinio, P. *J. Chem. Phys.* **1986**, *84*, 5102.
(22) Provencher, S. W. *Makromol. Chem.* **1979**, *180*, 201.
(23) Jakeš, J. *Czech. J. Phys. B.* **1988**, *38*, 1305.
(24) Schwartzl, F. R. *Pure Appl. Chem.* **1970**, *23*, 219.
(25) Candau, S. J.; Butler, T. A.; King, T. A. *Polymer* **1983**, *24*, 1601.
(26) Corrections are made for backflow as described in ref 6 where the concentration dependence of $D_e(6\pi\eta_s/kT)$, which is equal to ξ_e^{-1} in the terminology used here, is discussed.
(27) Brochard, F.; de Gennes, P.-G. *Macromolecules* **1977**, *10*, 1157.
(28) Brochard, F. *J. Phys. (Paris)* **1983**, *44*, 39.
(29) Štěpánek, P.; Koňák, C.; Sedlaček, B. *Macromolecules* **1982**, *15*, 1214.
(30) Adam, M.; Delsanti, M. *J. Phys. (Les Ulis, Fr.)* **1984**, *45*, 1513.
(31) Nicolai, T.; Brown, W.; Johnsen, R. M. *Macromolecules* **1989**, *22*, 2795.
(32) Zimm, B. H. *J. Chem. Phys.* **1956**, *24*, 269.
(33) Miyaki, Y.; Einada, Y.; Fujita, H. *Macromolecules* **1980**, *3*, 588.
(34) Chu, B., personal communication.

Registry No. PS, 9003-53-6.